

Long-range ferroelectric interactions in $\text{KTaO}_3/\text{KNbO}_3$ superlattice structures

H.-M. Christen,^{a)} E. D. Specht, D. P. Norton, M. F. Chisholm, and L. A. Boatner^{b)}
Oak Ridge National Laboratory, Oak Ridge, Tennessee 37831

(Received 27 February 1998; accepted for publication 17 March 1998)

Symmetric superlattice structures consisting of alternating atomic-scale layers of KTaO_3 and KNbO_3 with variable periodicity were grown on KTaO_3 substrates by pulsed laser deposition. The in-plane structure of KNbO_3 closely matches that of the KTaO_3 substrate, resulting in $\text{KTaO}_3/\text{KNbO}_3$ heterostructures that are uniformly strained in-plane without misfit dislocations. This strain imposes an in-plane KNbO_3 lattice spacing identical to that of the KTaO_3 substrate for the temperature range $30^\circ\text{C} < T < 700^\circ\text{C}$, and a tetragonal-to-tetragonal transition is observed whose phase transition temperature T_c depends on the KNbO_3 layer thickness. The in-plane strain results in a significant increase in this ferroelectric-paraelectric T_c for superlattices with relatively thick KNbO_3 layers ($T_c = 535^\circ\text{C}$ for a 17 nm thick layer, as compared to 435°C for bulk KNbO_3) and for $\text{K}(\text{Nb}_{0.5}\text{Ta}_{0.5})\text{O}_3$ random-alloy thin films. As the superlattice period decreases, a reduction of T_c is observed. For superlattices with periodicities of 50 Å or less, the Curie temperature is identical to that of the $\text{K}(\text{Ta}_{0.5}\text{Nb}_{0.5})\text{O}_3$ random-alloy film, indicating significant long-range ferroelectric coupling across the KTaO_3 layers. © 1998 American Institute of Physics. [S0003-6951(98)03720-6]

A number of attempts have been made to detect and quantify size effects in ferroelectric materials, but unequivocal observations of these phenomena have proven to be relatively elusive due primarily to a variety of experimental difficulties. Most recent experimental investigations have focused on the decrease of the ferroelectric phase transition temperature, T_c , as observed in fine-grained ceramics,^{1,2} the decrease of the ferroelectric domain size with decreasing thickness as observed in free-standing wedge-shaped transmission electron microscopy (TEM) samples,^{3,4} and on the increase of T_c in epitaxial thin films.^{5,6} Unfortunately, in all of these studies, either defects, surface charges, nonuniform strains, or other extrinsic effects have complicated the interpretation of the experimental results—thereby precluding a clear and unambiguous identification of intrinsic size effects.

In the present work, the difficulties noted above are circumvented by exploiting the special properties of epitaxial superlattices consisting of alternating layers of paraelectric KTaO_3 and ferroelectric KNbO_3 grown on (001)-oriented KTaO_3 substrates. Although a number of similar perovskite superlattices have been studied previously,^{7–11} the $\text{KTaO}_3/\text{KNbO}_3$ system is distinguished from these prior studies since the lattice mismatch between KNbO_3 and KTaO_3 at the growth temperature is less than 1.5%. If superlattices can be grown without the formation of misfit dislocations, the strain in the films will be uniform and independent of the layer thickness, providing an excellent system in which an unambiguous study of size effects in ferroelectrics can be made.

Superlattice layers of KTaO_3 and KNbO_3 were grown by pulsed laser deposition as reported previously.¹² All of the

superlattices were grown *in situ* to a total thickness of 170 nm. For comparison purposes, a 170 nm thick film of the solid solution $\text{KTa}_{0.5}\text{Nb}_{0.5}\text{O}_3$ was also grown as described in Ref. 13. Atomically flat substrates (as examined in Ref. 14) were used in all cases.

The $\text{KTaO}_3/\text{KNbO}_3$ superlattice structures were initially analyzed by Z-contrast scanning transmission electron microscopy (STEM)¹⁵ using [100] zone-axis-oriented cross-sectional samples. Figure 1(a) shows that the interfaces between 4 unit-cell-thick KTaO_3 layers and 3 unit-cell-thick KNbO_3 layers are atomically sharp. No misfit dislocations were observed in any portion of the TEM specimen. The image shown in Fig. 1(b) demonstrates the continuity of the superlattice. The TEM images were used to calibrate the growth rates for the KTaO_3 and KNbO_3 layers. All of the samples that were subsequently analyzed were grown with equal thicknesses of both constituents.

The crystallographic structure of the $\text{KTaO}_3/\text{KNbO}_3$ superlattices was investigated by x-ray diffraction (XRD) using a four-circle diffractometer and a $\text{Cu } K_{\alpha 1}$ source. Radial θ - 2θ scans show superlattice satellite peaks as illustrated in Fig. 2, from which the thickness of each superlattice period could be determined accurately. In the five samples investigated, the thickness of each layer measures: 169 Å (≈ 42 unit cells), 51 Å (≈ 13 unit cells), 24 Å (≈ 6 unit cells), 15.8 Å (≈ 4 unit cells), and 4 Å (≈ 1 unit cell), respectively.

None of the samples investigated here exhibited split peaks in the x-ray ϕ scans. Thus, no sign of an orthorhombic structure was found—contrary to the results of observations reported previously for 1660 Å thick films.¹² The observed peaks are consistent with a tetragonal structure in which the [100] and [010] axes of the film are parallel to those of the substrate, and the [001] direction is normal to the film surface. The in-plane lattice parameter a of all of these films is

^{a)}Present address: Neocera, Inc., 1000 Virginia Manor Rd., Suite 300, Beltsville, MD 20705-4125.

^{b)}Electronic mail: lb4@ornl.gov

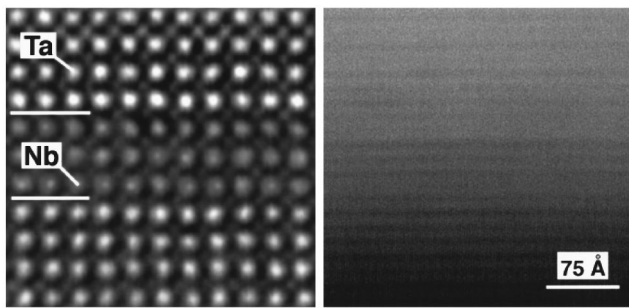


FIG. 1. (Left) Atomic-resolution Z-contrast scanning transmission electron micrograph of a superlattice consisting of KTaO_3 layers (each 4 unit-cells-thick) and KNbO_3 layers (each 3 unit-cells-thick). The distance between the centers of the Ta rows and columns corresponds to the 3.989 Å unit-cell dimension of KTaO_3 . This image demonstrates the sharpness of the superlattice interfaces. (Right) Lower-magnification Z-contrast image of the same sample illustrating the continuity of the superlattice as observed throughout the entire sample.

identical to that of the KTaO_3 substrate within the experimental resolution of 0.05%.

The results of the present work, combined with those reported in our previous study,¹² show that KNbO_3 films grown on KTaO_3 substrates exhibit three distinct room-temperature crystalline structures depending on the layer thickness d . For the thickest films ($d \geq 1.5 \mu\text{m}$), the orthorhombic (ambient temperature) phase of bulk KNbO_3 is recovered, whereas at intermediate thicknesses ($d \approx 1660 \text{ \AA}$), a different type of orthorhombic structure is observed. At the thicknesses investigated here ($d \leq 169 \text{ \AA}$), the KNbO_3 thin films are tetragonal.

Both the in-plane and out-of-plane lattice parameters of the $\text{KTaO}_3/\text{KNbO}_3$ superlattices were measured as a function of temperature, and the results are shown in Fig. 3(a). No thermal hysteresis is observed in any of the films, and only the data obtained on cooling is shown for clarity. Also depicted is the in-plane lattice parameter of the substrate. Clearly, the films remain fully “clamped” to the substrate at all temperatures and are thus homogeneously strained. This strain is independent of the layer thickness for the films considered.

A change-of-sign is observed in the out-of-plane thermal expansion of the film at a temperature T_c , indicating a phase

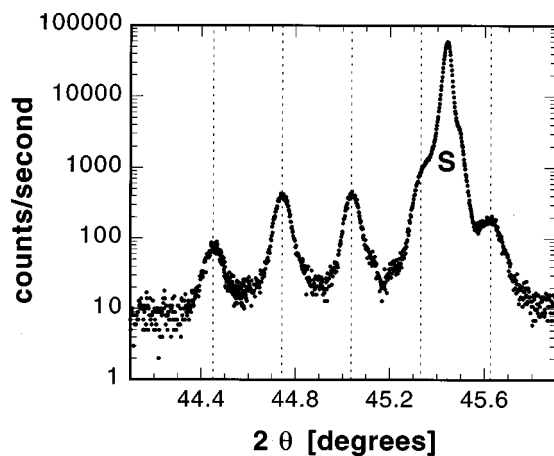


FIG. 2. X-ray θ - 2θ scan through the (002) Bragg peak for a $\text{KTaO}_3/\text{KNbO}_3$ superlattice showing satellite peaks from which the periodicity of the superlattice can be determined to be 33.8 nm. S indicates the substrate (002) peak.

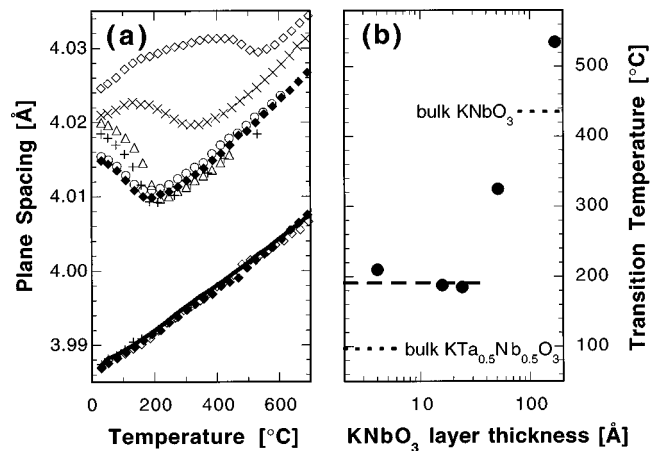


FIG. 3. (a) Lattice parameter of the $\text{KTaO}_3/\text{KNbO}_3$ superlattices as a function of temperature. Only data obtained on cooling is shown for clarity. The out-of-plane lattice constant is shown for superlattices with KNbO_3 layer thicknesses of 169 Å (\diamond), 51 Å (\times), 24 Å (\circ), 15.8 Å (\blacklozenge), and 4 Å (\triangle), as well as for a solid-solution film ($+$). For clarity, the in-plane lattice parameter is only shown for the 169 Å (\diamond) and 15.8 Å (\blacklozenge) superlattices as well as the solid-solution ($+$), and compared to that of the substrate (solid line). (b) Transition temperature as a function of KNbO_3 layer thickness. The broken line indicates the transition temperature of the solid-solution film. Also shown are the transition temperatures of bulk KNbO_3 and $\text{KTa}_{0.5}\text{Nb}_{0.5}\text{O}_3$ for comparison.

transition. The T_c for this tetragonal-to-tetragonal transition is plotted as a function of layer thickness in Fig. 3(b) and compared to that of the solid-solution film (subject to the same in-plane clamping as the superlattices) and the transition temperatures of bulk KNbO_3 and $\text{KTa}_{0.5}\text{Nb}_{0.5}\text{O}_3$.¹⁶ Only one phase transition is observed above room temperature in these films, whereas bulk KNbO_3 undergoes two transitions (from orthorhombic to tetragonal and from tetragonal to cubic). As Fig. 3(b) shows, for the thickest KNbO_3 layers ($d = 169 \text{ \AA}$), the transition temperature ($T_c = 535 \text{ }^\circ\text{C}$) lies above that of bulk KNbO_3 ($T_c = 435 \text{ }^\circ\text{C}$). It appears that this increase in T_c is strain-induced. The same strain-induced increase in T_c is observed in the $\text{KTa}_{0.5}\text{Nb}_{0.5}\text{O}_3$ film ($T_c = 190 \text{ }^\circ\text{C}$, whereas $T_c = 93 \text{ }^\circ\text{C}$ for the bulk).¹⁶ This strain-induced increase in T_c is not surprising. At the transition temperature of bulk KNbO_3 (435 °C), the substrate lattice parameter is $a = 4.000 \text{ \AA}$ [Fig. 3(a)]. Using published values for the lattice constant of cubic and tetragonal KNbO_3 ,¹⁷ and assuming a similar thermal expansion for KNbO_3 as for KTaO_3 [taken from Fig. 3(a)], one finds for KNbO_3 at 435 °C, $a_{\text{cubic}} = 4.005 \text{ \AA}$ and $a_{\text{tetragonal}} = 4.002 \text{ \AA}$. Because the tetragonal structure is a better match to the KTaO_3 substrate, the “clamping” effect to the substrate will tend to stabilize the low-temperature phase above the bulk phase transition.

Our experimental observations are consistent with those for BaTiO_3 films⁴ and are supported by calculations based on the Landau theory of ferroelectricity.¹⁸ The present work demonstrates that, in fact, the increase in T_c results from strain rather than from interface defects. It is anticipated that this “clamping” technique could be applied to other ferroelectric films in order to obtain the higher transition temperatures desired for many sensor applications.¹⁹

As the periodicity of the $\text{KTaO}_3/\text{KNbO}_3$ superlattice decreases, a reduction of T_c is observed. It is worthwhile to note that a similar behavior occurs in the case of a free-

standing ferroelectric slab in order to minimize simultaneously the depolarization energy and the domain wall energy.^{20,21} The boundary conditions for the KNbO₃ films in the present superlattices are, however, different from those encountered in the case of a single ferroelectric film in vacuum. Nevertheless, considering the experimental difficulties encountered in distinguishing between extrinsic (surface charges, defects, etc.) and intrinsic size effects in other types of experiments,^{1–6} the present superlattices provide an important alternative approach to study the underlying mechanisms, as is further explored elsewhere.²² A model proposed by Schwenk *et al.*²³ considers a multilayer system consisting of two soft-mode-driven ferroelectrics with different transition temperatures. (Note that KTaO₃ can be regarded as a soft-mode type ferroelectric with a hypothetical transition temperature low enough to be suppressed by zero-point fluctuations.²⁴) The results of a Ginzburg–Landau functional calculation indicate that with decreasing thickness of the individual layers, the transition temperature decreases, as is also found in numerical simulations treating the system as a transverse Ising model.²⁵

An interesting observation made in the present study is that the symmetric KTaO₃/KNbO₃ superlattice structures with periodicities below 50 Å mimic the behavior of a random K(Ta_{0.5}Nb_{0.5})O₃ alloy. This is observed despite the fact that both cross-sectional Z-contrast STEM and XRD indicate little or no interdiffusion of the layers. Note that the transition being considered involves a *c*-axis distortion, and that the in-plane structure is independent of the superlattice structure. At these thicknesses, the experimental methods employed do not allow us to distinguish between the *c*-axis lattice constant of the individual KTaO₃ and KNbO₃ layers. These lattice parameters could—in principle—be different, whereas in the case of the random alloy, one *c*-axis lattice parameter suffices to describe the crystal structure. From the observation of “alloylike” behavior in the superlattices, we conclude that for superlattice periodicities below 50 Å, the KTaO₃ and KNbO₃ layers cease to behave independently of each other. This is a clear indication of the long-range nature of the ferroelectric interactions.

With an absence of defects and with a strain that is independent of the layer thickness, KTaO₃/KNbO₃ multilayers have proven to be an excellent system for the study of size effects, strain effects, and long-range ferroelectric interactions. The following three conclusions summarize our findings: (1) uniform compressive strain results in an increase of T_c in KNbO₃, (2) decreasing the superlattice period in symmetric KTaO₃/KNbO₃ superlattice structures results in a de-

crease of T_c , and (3) a critical length scale of ~ 50 Å is observed, below which superlattices behave as a random alloy film of the same average composition, illustrating the long-range nature of ferroelectric interactions in the KTaO₃/KNbO₃ system.

The authors acknowledge the help of J. A. Kolopus, J. T. Luck, P. Menchhofer, J. O. Ramey, and M. Urbanik (Commercial Crystal Laboratories, Inc.). This research was sponsored by the Division of Materials Sciences, U.S. Department of Energy under Contract No. DE-AC05-96OR22464 with Lockheed Martin Energy Research Corp., and in part by an appointment to the Oak Ridge National Laboratory Postdoctoral Research Associates Program.

¹M. H. Frey and D. A. Payne, Appl. Phys. Lett. **63**, 2753 (1993).

²P. Ayyub, V. R. Palkar, S. Chattopadhyay, and M. Multani, Phys. Rev. B **51**, 6135 (1995); S. Chattopadhyay, P. Ayyub, V. R. Palkar, and M. Multani, *ibid.* **52**, 13177 (1995).

³F. Tsai and J. M. Cowley, Appl. Phys. Lett. **65**, 1906 (1994).

⁴S. B. Ren, C. J. Lu, J. S. Liu, H. M. Shen, and Y. N. Wang, Phys. Rev. B **54**, R14337 (1996).

⁵I. N. Zakharchenko, E. S. Nikitin, V. M. Mukhortov, Yu. I. Golovko, M. G. Gadchenko, and V. P. Dudkevich, Phys. Status Solidi A **114**, 559 (1989).

⁶Y. Yano, K. Iijima, Y. Daitoh, T. Terashima, and Y. Bando, J. Appl. Phys. **76**, 7833 (1994).

⁷E. Wiener-Avneer, Appl. Phys. Lett. **65**, 1784 (1994).

⁸H. Tabata, H. Tanaka, and T. Kawai, Appl. Phys. Lett. **65**, 1970 (1994).

⁹H. Tabata and T. Kawai, Appl. Phys. Lett. **70**, 321 (1997).

¹⁰A. Erbil, Y. Kim, and R. A. Gerhardt, Phys. Rev. Lett. **77**, 1628 (1996).

¹¹I. Kanno, S. Hayashi, R. Takayama, and T. Hirao, Appl. Phys. Lett. **68**, 328 (1996).

¹²H.-M. Christen, L. A. Boatner, J. D. Budai, M. F. Chisholm, L. A. Géa, P. J. Marrero, and D. P. Norton, Appl. Phys. Lett. **68**, 1488 (1996).

¹³H.-M. Christen, D. P. Norton, L. A. Géa, and L. A. Boatner, Thin Solid Films **312**, 162 (1998).

¹⁴H.-M. Christen, L. A. Boatner, J. D. Budai, M. F. Chisholm, L. A. Géa, D. P. Norton, Ch. Gerber, and M. Urbanik, Appl. Phys. Lett. **70**, 2147 (1997).

¹⁵S. J. Pennycook and D. E. Jesson, Phys. Rev. Lett. **64**, 938 (1990).

¹⁶D. Rytz and H. J. Scheel, J. Cryst. Growth **59**, 468 (1982).

¹⁷A. W. Hewat, J. Phys. C: Solid State Phys. **6**, 2559 (1973).

¹⁸J. S. Zhu, X. M. Lu, P. Li, W. Jiang, and Y. N. Wang, Solid State Commun. **101**, 263 (1996).

¹⁹R. C. Turner, P. A. Fuierer, R. E. Newnham, and T. R. Shrout, Appl. Acoustics **41**, 299 (1994).

²⁰M. E. Lines and A. M. Glass, *Principles and Applications of Ferroelectrics and Related Materials* (Clarendon, Oxford, 1977), p. 94.

²¹Y. G. Wang, W. L. Zhong, and P. L. Zhang, Phys. Rev. B **51**, 5311 (1995).

²²E. D. Specht, H.-M. Christen, D. P. Norton, and L. A. Boatner, Phys. Rev. Lett. (to be published).

²³D. Schwenk, F. Fishman, and F. Schwabl, Phys. Rev. B **38**, 11618 (1988); J. Phys.: Condens. Matter **2**, 5409 (1990).

²⁴U. T. Höchli and L. A. Boatner, Phys. Rev. B **20**, 266 (1979).

²⁵B. D. Qu, W. L. Zhong, and P. L. Zhang, Phys. Lett. A **189**, 419 (1994); Jpn. J. Appl. Phys., Part 1 **34**, 4114 (1995).